Von Neumann stability analysis of the upwind finite difference schemes

Erwan Deriaz* and Pierre Haldenwang†

July 26, 2013

Abstract

This paper presents finite-difference stability issues for the simulation of convection dominated problems. Its main objective is to provide original and accurate CFL-like stability conditions for a large collection of finite-difference schemes thanks to von Neumann stability analysis. In particular, we exhibit a wide variety of stability conditions of the type $\Delta t \leq C\Delta x^\alpha$ with Δt the time step, Δx the space step, and for $\alpha \in [1, 2]$. This result was announced in [5], here we detail and prove it. Some numerical experiments illustrate these theoretical results.

Introduction

The aim of this paper is to prospect the stability conditions coming from the von Neumann stability analysis of the transport equation with finite difference discretizations. One could think that this topic is well known, but he would be surprised by the variety of existing CFL-like stability conditions which are evidenced here.

Further on, we denote the time step by Δt, the space step by Δx and the velocity by a. When a is omitted then Δx stands for $\Delta x/a$. The CFL condition which is a physical criterion [3], asserts that in presence of a transport phenomenon at speed a these parameters have to satisfy $\Delta t \leq C\,\Delta x/a$ with C a constant close to 1, in order to provide physical relevance, and it is a necessary condition for the numerical stability of explicit schemes.

Nevertheless, the linear CFL condition may not be sufficient to ensure the numerical stability. Thanks to the von Neumann stability analysis [1], we prove that there exist possible stability conditions of the type $\Delta t \leq C\,\Delta x^\alpha$ with $\alpha \in [1, 2]$ a rational number. This exponent α is given by $\alpha = \frac{p(2q-1)}{q(2p-1)}$ with p and q non zero natural numbers with $q \geq p$.

The organization of the paper is the following: in the first part we briefly review the stability domain of the time schemes, mainly studied for the ordinary differential equation theory and brilliantly presented in references [8, 9], in the second part we discuss the spectra of the finite difference approximations, in the third part, we combine these two elements to make our stability condition $\Delta t \leq C\,\Delta x^\alpha$ appear, and in the fourth part we test this condition numerically.

*Institut Jean Lamour, Faculté des Sciences et Technologies, Campus Victor Grignard - BP 70239, 54506 VANDOEUVRE-LES-NANCY (France), erwan.deriaz@l3m.univ-mrs.fr

†Laboratoire de Mécanique, Modélisation et Procédés Propres, 38 rue Frédéric Joliot-Curie 13451 MARSEILLE Cedex 20 (France), haldenwang@l3m.univ-mrs.fr

1 Stability domain of the time schemes

Solving differential equations by the use of numerical schemes has a utter importance in nowadays technology [7], and was exhaustively explored in the case of ordinary differential equations [8, 9]. We will briefly review some theoretical elements about the numerical stability of usual schemes here.

Let us consider the differential equation

$$\partial_t u = F(u), \quad t \geq 0. \tag{1.1}$$

To solve this equation numerically, one can use a one step scheme –i.e. a scheme of Runge-Kutta type:

$$u_{(i)} = u_n + \Delta t \sum_{j=0}^{i-1} a_{ij} F(u_{(j)}), \quad \text{for } 0 \leq i \leq s, \quad \text{and } u_{n+1} = u_{(s)}, \tag{1.2}$$

where u_n is an approximation of the solution u at time $n\,\Delta t$.
Or, one can use a multistep scheme [13] which is written:

$$u_{n+1} = \sum_{i=0}^{r} a_i u_{n-i} + \Delta t \sum_{i=0}^{s} b_i F(u_{n-i}). \tag{1.3}$$

Depending on the choice of the coefficients a_{ij} or a_i and b_i, the numerical scheme will have a certain accuracy and certain stability features.

In order to describe some stability properties of these schemes, we consider the differential equation $\partial_t u = \zeta\, u$ –i.e. the case $F(u) = \zeta\, u$– with $\zeta \in \mathbb{C}$. Then the scheme (1.2) satisfies

$$u_{n+1} = G(z) u_n, \tag{1.4}$$

where $z = \zeta\, \Delta t$. The polynomial function G is called the amplification factor.
For multistep schemes, the definition of the amplification factor has to be more general. Let

$$X_n = \begin{pmatrix} u_n \\ u_{n-1} \\ \vdots \\ u_{n-s} \end{pmatrix}, \tag{1.5}$$

then the scheme (1.3) corresponds to $X_{n+1} = M(z) X_n$, where $M(z)$ is a $(s+1) \times (s+1)$ matrix. As $X_{i+n} = M(z)^n X_i$, we will be interested in the eigenvalues of $M(z)$ and particularly in the one with maximal norm. Hence, in the multistep case, $|G(z)|$ stands for the maximum of the norms of the eigenvalues.

In the theory of ordinary differential equations [8], the von Neumann stability domain gathers all the points $z \in \mathbb{C}$ where the amplification factor is less than one:

$$\mathcal{D} = \{z \in \mathbb{C}, |G(z)| \leq 1\}. \tag{1.6}$$

In Fig. 1 we represented the stability domains of the first four Runge-Kutta schemes and of a Runge-Kutta scheme of order 5 taken from the numerical analysis manual [4].

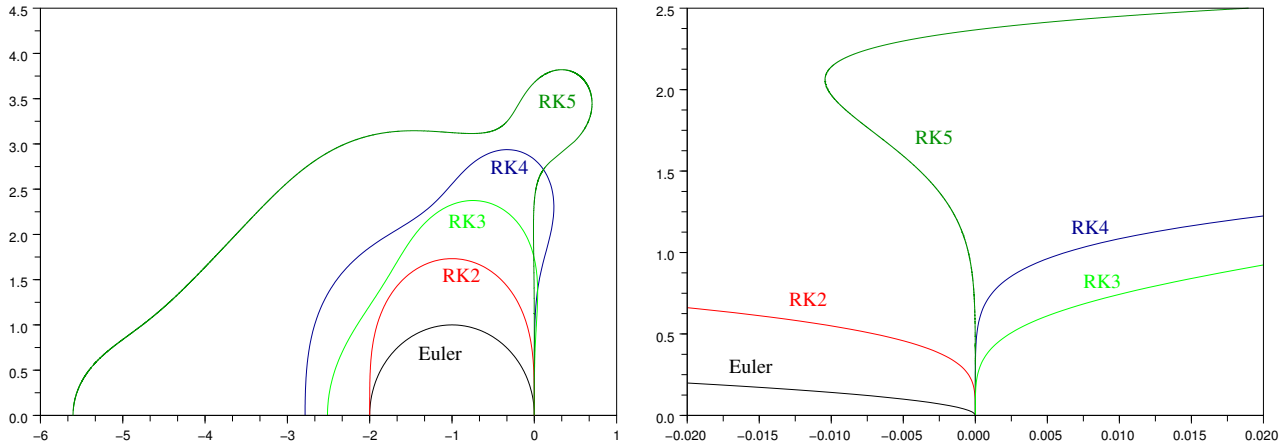

Runge-Kutta zoom along (Ox)

Figure 1: Von Neumann stability domains for first five Runge-Kutta schemes. Left: on the half-plan. Right: zooming in the x direction. The fifth Runge-Kutta scheme is taken from [4].

When we have to deal with partial differential equations, the semi-discretization of the equations (only in space, and not in time), and their diagonalization (when it is possible) stem to multiple ordinary differential equations. For instance, the transport equation

$$\partial_t u - a\partial_x u = 0, \quad (t,x) \in [0,T] \times \mathbb{T}$$

for $a \in \mathbb{R}$ given and $u : \mathbb{T} \to \mathbb{R}$ the unknown, when using a Fourier spectral discretization in space stems to

$$\partial_t \hat{u} - ia\xi\hat{u} = 0, \quad t \in [0,T]$$

for each wave number $\xi \in 2\pi[-N/2, N/2]$ of the discretization:

$$u(t,x) = \sum_{\xi=-N/2}^{N/2} \hat{u}(t,\xi)\, e^{i\xi x}.$$

So the time scheme is stable for the transport equation if $ia\xi \in \mathcal{D}$ for $\xi \in 2\pi[-N/2, N/2]$.

Hence the inclusion of the (Oy) axis into $\mathcal{D}$ near zero, informs on the behavior of the schemes for simulating transport-dominated equations: if $\partial\mathcal{D}$ goes to the right (RK3, RK4) then the scheme is stable under linear CFL condition $\Delta t \leq C\Delta x$, and if $\partial\mathcal{D}$ goes to the left (Euler, RK2, RK5) then the stability needs a stronger CFL condition $\Delta t \leq C\Delta x^\alpha$ with $\alpha > 1$ [5, 6].

In Fig. 2 we show the stability domains of the first five Adams-Bashforth schemes. According to the behavior of the tangencies along the (Oy) axis, we can say that the schemes AB3 and AB4 are stable under the usual linear CFL condition while the schemes Euler, AB2 and AB5 are not.

In our study, we will be particularly interested in the behavior of the boundary of the stability domain $\mathcal{D}$ which is embedded in $\{z \in \mathbb{C} \text{ s.t. } G(z) = e^{i\theta}, \theta \in (-\pi, \pi]\}$, and more

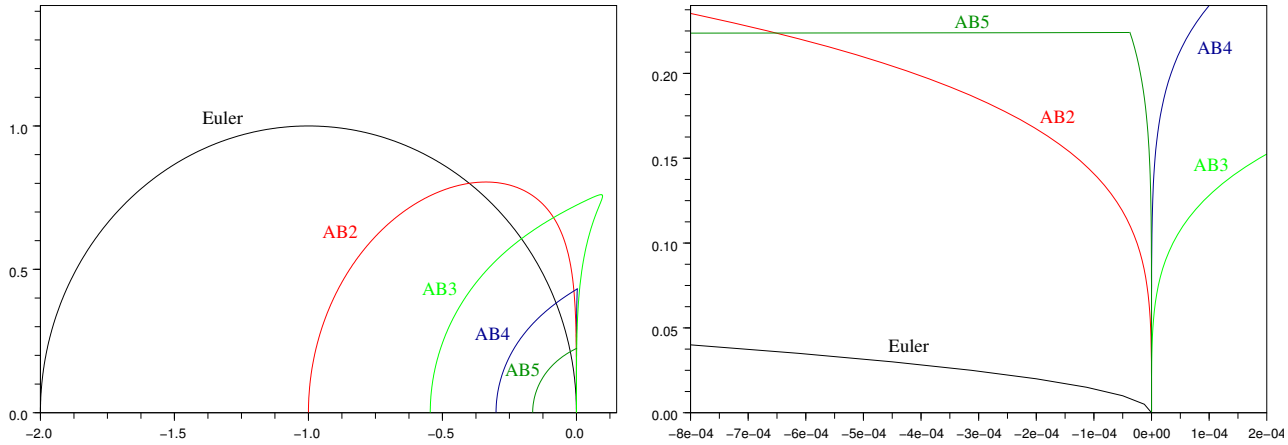

Adams-Bashforth zoom along (Ox)

Figure 2: Von Neumann stability domains for the first five Adams-Bashforth schemes. Left: on the half-plan. Right: zooming in the x direction.

particularly to the boundary of $\mathcal{D}$ near $z = 0$.
Actually, in a neighborhood of zero, the boundary of $\mathcal{D}$ satisfies:

$$z = i(\theta + o(\theta)) - T_{\mathcal{D}}\theta^{2p} + o(\theta^{2p}), \quad \theta \in \mathbb{R}, \quad \theta \text{ close to } 0. \tag{1.7}$$

The parameters $p \in \mathbb{N}$ and $T_{2p} \in \mathbb{R}$ are computed from the coefficients of the polynomial $G(z)$ for the one step schemes, or by writing directly that $e^{i\theta}$ is an eigenvalue of $M(z)$ for the multistep schemes (see [5] for more details).

2 Space differentiation

2.1 Spectrum of the discrete differentiation

Finite differences originate from the approximation of functions by polynomials, with a first appearance in Newton's notes as early as the seventeenth century [10]. And nowadays, their applications are widely spread in numerical simulations and particularly in computational fluid dynamics [12]. The reader can report to [14] for an extensive introduction to finite difference approximations.

We consider the problem of approximating the pointwise differentiation of a function. This operation modifies the spectrum of the differential operator –contrarily to a spectral discretization. Given a smooth function $u : \mathbb{R} \to \mathbb{R}$ discretized on a regular space grid $\{k\,\Delta x, k \in \mathbb{Z}\}$, we approximate $\partial_x u(x)$ for $x \in \Delta x\mathbb{Z}$ using the points $\{x - m\,\Delta x, \ldots, x + n\,\Delta x\}$ for $m, n \in \mathbb{N}$ –i.e. the stencil [-m,n]– by:

$$A\,u(x) = \frac{1}{\Delta x} \sum_{k=-m}^{n} a_k u(x + k\,\Delta x) \tag{2.1}$$

where the operator A denotes a discrete differentiation approximating ∂_x.

The spectrum of A can be obtained by taking $u(x) = e^{\frac{i\xi x}{\Delta x}}$, then $A\,u(x) = \frac{1}{\Delta x} A(\xi)\,u(x)$ with

$$A(\xi) = \sum_{k=-m}^{n} a_k e^{ik\xi}, \quad \xi \in [-\pi, \pi]. \tag{2.2}$$

We plot this spectrum on the plan of complex numbers by considering the curve

$$\mathcal{S} = \{A(\xi), \xi \in [-\pi, \pi]\} \subset \mathbb{C}. \tag{2.3}$$

It presents an axial symmetry along (Ox).

To be consistent, the discrete differentiation A has to satisfy $A(u)(x) = \partial_x u(x) + O(\Delta x)$ i.e.

$$\left\{ \begin{array}{l} \sum_k a_k = 0 \\ \sum_k k\, a_k = 1 \end{array} \right. \quad \text{which corresponds to} \quad \left\{ \begin{array}{l} A(0) = 0 \\ A'(0) = i \end{array} \right. . \tag{2.4}$$

The other interesting properties are listed below:

- the first and most important issue is the order of the approximation. An approximation A is said to be consistent of order β if it satisfies

$$\exists C > 0, \quad \forall u \in C_0^\infty, \quad \|\partial_x u - Au\|_{L^2} \leq C\, \Delta x^\beta\, \|\partial^{\beta+1} u\|_{L^2}, \tag{2.5}$$

- another important issue affects the stability with respect to the time integration: the upwind or downwind feature of a scheme. A necessary condition for the time integration to be stable is that the spectrum of the differentiation have no strictly positive real part i.e. $\mathcal{S} \subset \mathbb{C}^- = \{\xi \in \mathbb{C}, \mathrm{Re}\, \xi \leq 0\}$, see Fig. 3. For centered finite differences, we have $\mathcal{S} \subset i\mathbb{R}$.

- and finally, another important issue, essential for the present article, regards the conservativity of the space discretization. The conservativity of a differentiation is linked to the tangency of its spectrum $\mathcal{S}$ to the (Oy) axis:

$$A(\xi) = i\,(\xi + o(\xi)) - T_{\mathcal{S}}\, \xi^{2q} + o(\xi^{2q}) \tag{2.6}$$

  with $q \in \mathbb{N}^*$ and $T_{\mathcal{S}} > 0$.

The link between the numbers q and $T_{\mathcal{S}}$ and the conservativity goes as follows: let us assume that we are using a differentiation A satisfying (2.6), then the method of lines (i.e. considering exclusively the space discretization) transforms the transport equation $\partial_t u = \partial_x u$, into $\partial_t \hat{u}(\xi) = \Delta x^{-1} A(\xi\, \Delta x)\hat{u}(\xi)$. The solution of this equation is given by $\hat{u}(t, \xi) = \exp(\Delta x^{-1} A(\xi\, \Delta x)t)\hat{u}(0, \xi)$. So, for $\Delta x \to 0$, according to (2.6), the damping of the frequency ξ may be approximated by

$$\begin{aligned} |\hat{u}(t, \xi)| &= \exp(-T_{\mathcal{S}}\, \xi^{2q}\, \Delta x^{2q-1}\, t + o(\Delta x^{2q-1}))|\hat{u}(0, \xi)| & (2.7) \\ &= (1 - T_{\mathcal{S}}\, \xi^{2q}\, \Delta x^{2q-1}\, t + o(\Delta x^{2q-1}))|\hat{u}(0, \xi)|. & (2.8) \end{aligned}$$

The multiplicative factor goes to 1 faster for larger q allowing a better conservation of the energy.

2.2 Most conservative differentiations

For further experiments, we look for discretized differentiations A maximizing the tangency of the spectrum to the (Oy) axis, i.e. maximizing the number q in the expression (2.6). From (2.2), we deduce:

$$A(\xi) = \sum_{k=-m}^{n} a_k e^{ik\xi} = \sum_{k=-m}^{n} a_k \sum_{\ell \geq 0} \frac{(ik\xi)^\ell}{\ell!} = \sum_{\ell \geq 0} \frac{i^\ell}{\ell!} \left(\sum_{k=-m}^{n} a_k k^\ell \right) \xi^\ell. \tag{2.9}$$

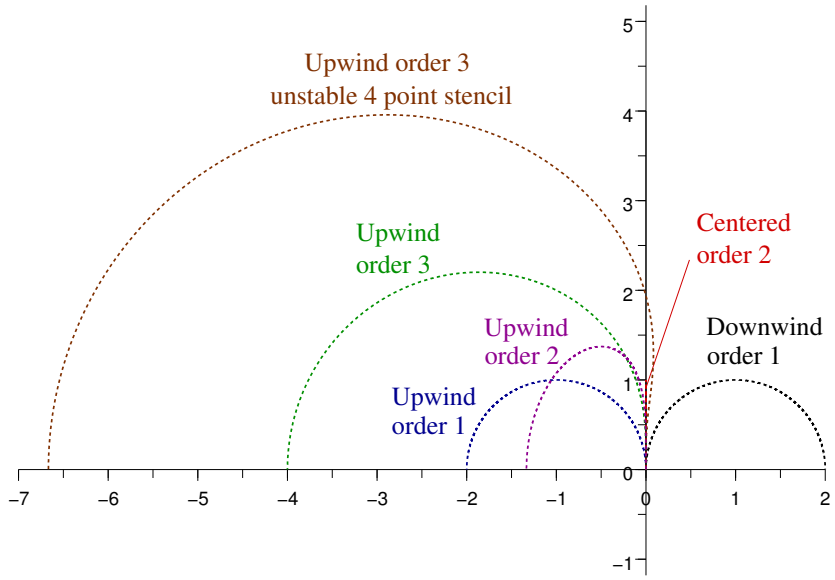

Figure 3: Spectra of several finite difference schemes for space differentiation. These spectra have to be compared with the domains of stability of the temporal schemes Fig. 1 and 2.

Maximizing the order of the approximation is equivalent to solving the system of equations

$$\sum_{k=-m}^{n} a_k = 0 \tag{2.10}$$

$$\sum_{k=-m}^{n} k\, a_k = 1 \tag{2.11}$$

$$2 \leq \ell \leq s, \quad \sum_{k=-m}^{n} k^\ell a_k = 0 \tag{2.12}$$

for $s = m + n$, so this provides an order s approximation. A finite differentiation is stable if its spectrum shows no strictly positive real part. Thanks to numerical experiments, we have noticed two features: if s is odd –i.e. with an even number of points– there is only one stencil providing an order s stable finite differentiation, if s is even, there are two of them; and for each s, one stable instance corresponds to an upwind scheme, and the other –for s even– to a centered scheme.
In order to maximize the tangency of $\mathcal{S}$ to the (Oy) axis, we extract the real part of the polynomial expansion of $A(\xi)$ (2.9). As a result, only the equalities (2.4) and (2.12) with

even parameter ℓ enter into play:

$$\ell = 0, \quad \sum_{k=-m}^{n} a_k = 0 \tag{2.13}$$

$$\ell = 1, \quad \sum_{k=-m}^{n} k\, a_k = 1 \tag{2.14}$$

$$2 \leq 2\ell \leq 2(q-1), \quad \sum_{k=-m}^{n} k^{2\ell} a_k = 0 \tag{2.15}$$

If $a_{-k} = -a_k$, then the scheme is centered and $q = +\infty$. If it is not the case, then we have an expansion of the type:

$$A(\xi) = i\,\xi + o(i\,\xi) + \left(\frac{(-1)^q}{(2q)!} \sum_{k=-m}^{n} k^{2q} a_k \right) \xi^{2q} + o(\xi^{2q}). \tag{2.16}$$

From (2.9), the real part of $A(\xi)$ is given by:

$$f(\xi) = \mathrm{Re}(A(\xi)) = a_0 + \sum_{k=1}^{N} (a_k + a_{-k}) \cos(k\,\xi) \tag{2.17}$$

with $N = \max(n, m)$ and (a_k) completed by $a_k = 0$ when k does not remain to the stencil. In the following we consider that $N = n$. We maximize the number of vanishing derivatives of f at zero, by taking

$$f(\xi) = -K_{m,n}(1 - \cos\xi)^n, \tag{2.18}$$

with $K_{m,n}$ a positive constant for $n \geq m$. With this choice, $q = n$ in the expansion (2.16).

Remark 1: This form for the real part of $A(\xi)$ maximizes the tangency to the (Oy) axis. And, since it does not contain any strictly positive value, it provides a stable upwind differentiation.

For $m = 0$, this leads to the unique solution $K_{0,n} = \frac{2^{n-1}}{\mathrm{C}_{2n-2}^{n-1}}$, $a_0 = -\frac{\mathrm{C}_{2n}^{n}}{2\,\mathrm{C}_{2n-2}^{n-1}}$ and $a_k = (-1)^{k+1} \frac{\mathrm{C}_{2n}^{n+k}}{\mathrm{C}_{2n-2}^{n-1}}$ for $k \geq 1$.
For the further numerical experiments, we will be using the case $m = n-1$ with maximum order of approximation (i.e. order $s = 2n-1$), leading to the coefficients of Table 1 for a velocity going from the right to the left: $\partial_t u + a\,\partial_x u = 0$ with $a < 0$.

Remark 2: For a finite number of points N with periodic boundary conditions, the Fourier modes of the simulation form a discrete set: $\{\xi = \pi \frac{k}{N},\ -N+1 \leq k \leq N\}$. That is why we plotted the spectrum of the discretized operator A with dotted lines in Fig. 3.

3 Stability condition $\Delta t \leq C\,\Delta x^{\alpha}$ with $\alpha > 1$

Gathering the information on the stability domain in one hand and on the spectrum of the discrete differentiation in the other hand, we are now able to state our main result on the von Neumann stability condition for upwind finite differences:

k / q	-4	-3	-2	-1	0	1	2	3	4	5
1					-1	1				
2				$-\frac{1}{3}$	$-\frac{1}{2}$	1	$-\frac{1}{6}$			
3			$\frac{1}{20}$	$-\frac{1}{2}$	$-\frac{1}{3}$	1	$-\frac{1}{4}$	$\frac{1}{30}$		
4		$-\frac{1}{105}$	$\frac{1}{10}$	$-\frac{3}{5}$	$-\frac{1}{4}$	1	$-\frac{3}{10}$	$\frac{1}{15}$	$-\frac{1}{140}$	
5	$\frac{1}{504}$	$-\frac{1}{42}$	$\frac{1}{7}$	$-\frac{2}{3}$	$-\frac{1}{5}$	1	$-\frac{1}{3}$	$\frac{2}{21}$	$-\frac{1}{56}$	$\frac{1}{630}$

Table 1: Upwind finite difference coefficients $(a_k)_{k\in[-m,n]}$ for several stencils $[-n, n+1]$. The resulting orders of approximation are equal to $2q-1$.

Theorem 3.1 *Let us consider a numerical solver for the transport equation $\partial_t u + a\,\partial_x u = 0$ using finite differences with time step Δt and space step Δx. If, close to zero, the boundary of the stability domain of the time integrator –noted $\mathcal{D}$ in (1.6)– satisfies:*

$$\partial\mathcal{D}: \quad z = i(\theta + o(\theta)) - T_{\mathcal{D}}\theta^{2p} + o(\theta^{2p}) \tag{3.1}$$

for $p \in \mathbb{N}$ and $T_{\mathcal{D}} > 0$, and if the spectrum $\mathcal{S} = \{A(\xi), \xi \in [-\pi, \pi]\}$ of the discrete differentiation –from (2.3)– satisfies:

$$\mathcal{S}: \quad z = i(\theta + o(\theta)) - T_{\mathcal{S}}\theta^{2q} + o(\theta^{2q}) \tag{3.2}$$

for $q \in \mathbb{N}$ and $T_{\mathcal{S}} > 0$, then the von Neumann stability condition

$$\|u_{n+1}\|_{L^2} \leq (1 + C\Delta t)\|u_n\|_{L^2} \tag{3.3}$$

of the numerical solution (u_n) is given by

$$\Delta t \leq C'\Delta x^{\alpha} \tag{3.4}$$

with $C' > 0$ a constant independent of Δt and Δx and with

- *$\alpha = 1$ if $q \leq p$ (stable under linear CFL condition),*
- *$\alpha = \frac{p(2q-1)}{(2p-1)q} \in (1, 2]$ if $q > p$, and in this case, the constant C' from (3.4) is written:*

$$C' = C^{\frac{q-p}{q(2p-1)}} \frac{T_{\mathcal{S}}^{\frac{p}{q(2p-1)}}}{T_{\mathcal{D}}^{\frac{1}{2p-1}}} \left(\left(\frac{p}{q}\right)^{\frac{p}{q-p}} - \left(\frac{p}{q}\right)^{\frac{q}{q-p}} \right)^{\frac{q-p}{q(2p-1)}}, \tag{3.5}$$

with p and $T_{\mathcal{D}}$ from (3.1), q and $T_{\mathcal{S}}$ from (3.2) and C from (3.3).

Remark 1: If $q = +\infty$ (centered schemes, spectral method) it makes appear the case presented in [5] for conservative space discretizations: $\alpha = \frac{2p}{2p-1}$.

Remark 2: The localization of all possible values of α is plotted in Fig. 4. It consists in accumulations from the left to the points of the sequence $(\frac{2p}{2p-1})_{p\geq 1}$. This sequence itself has an accumulation point at 1, from the right.

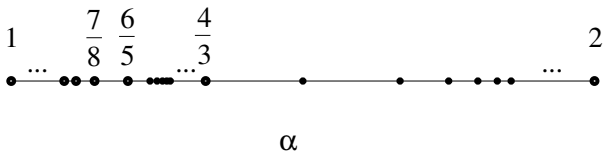

Figure 4: Possible locations of the exponent α.

Remark 3: Following Cockburn, Karniadakis and Shu [2], a Discontinuous Galerkin method combining an order two upwind scheme in space ($q = 2$) with a forward Euler scheme in time ($p = 1$) turns out to be stable under the condition $\Delta t \leq C\Delta x^{\alpha}$ (3.4) with the exponent $\alpha = \frac{3}{2}$, which explains why this numerical scheme "is stable if $\frac{\Delta t}{\Delta x}$ is of order $\sqrt{\Delta x}$".

Proof: We prove Theorem 3.1 directly by computation. It also corresponds to geometrical considerations: the spectrum $\frac{\Delta t}{\Delta x} \times \mathcal{S}$ must not get away from the domain of stability $\mathcal{D}$ by more than $C\Delta t$, see Fig. 5.

Geometrically, if $q \leq p$ then for $\tau = \frac{\Delta x}{\Delta t}$ sufficiently small the spectrum $\tau\mathcal{S}$ fits inside the stability domain $\mathcal{D}$. (The only exception occurs if $\mathcal{S} \cap i\mathbb{R} \neq \{0\}$.)

Let us consider the case $q > p$. The demonstration relies on the same computations as the demonstration of Theorem 3.1 of [5]. The tangency of the stability domain to the (Oy) axis, equation (3.1), corresponds to an amplification factor

$$G(z) = \beta_0 + \beta_1 z + \beta_2 z^2 + \dots \quad \text{such that} \quad |G(i\,\zeta)|^2 = 1 + 2T_{\mathcal{D}}\zeta^{2p} + o(\zeta^{2p}) \tag{3.6}$$

for $\zeta \in \mathbb{R}$ close to zero.

We are interested in the case that deviates a little from the spectral case $z \in i\,\mathbb{R}$, and we need to compute $|G(\frac{\Delta t}{\Delta x}A(\xi))|$ for $A(\xi) = i\xi - T_{\mathcal{S}}\xi^{2p} + o() \notin i\,\mathbb{R}$. We put $\tau = \frac{\Delta t}{\Delta x}$. Then $\tau A(\xi) = a + i\,b$ with $a = \tau Re(A(\xi)) = -T_{\mathcal{S}}\tau\,\xi^{2q} + o(\tau\,\xi^{2q})$ and $b = \tau Im(A(\xi)) = \tau\,\xi + o(\tau\,\xi)$ for $\xi \to 0$. As $\tau \to 0$ and $\xi \to 0$, a and b tends to zero with $a = o(b)$. Given that $\beta_0 = \beta_1 = 1$, we can write

$$G(a + i\,b) = 1 + (a + i\,b) + \beta_2(a + i\,b)^2 + \dots \tag{3.7}$$

then

$$\begin{aligned} |G(a + i\,b)|^2 &= (1 + a + \beta_2 a^2 - \beta_2 b^2)^2 + (b + 2\beta_2 a\,b)^2 + \dots && (3.8)\\ &= 1 + 2a - 2\beta_2 b^2 + \dots + b^2 + \dots && (3.9) \end{aligned}$$

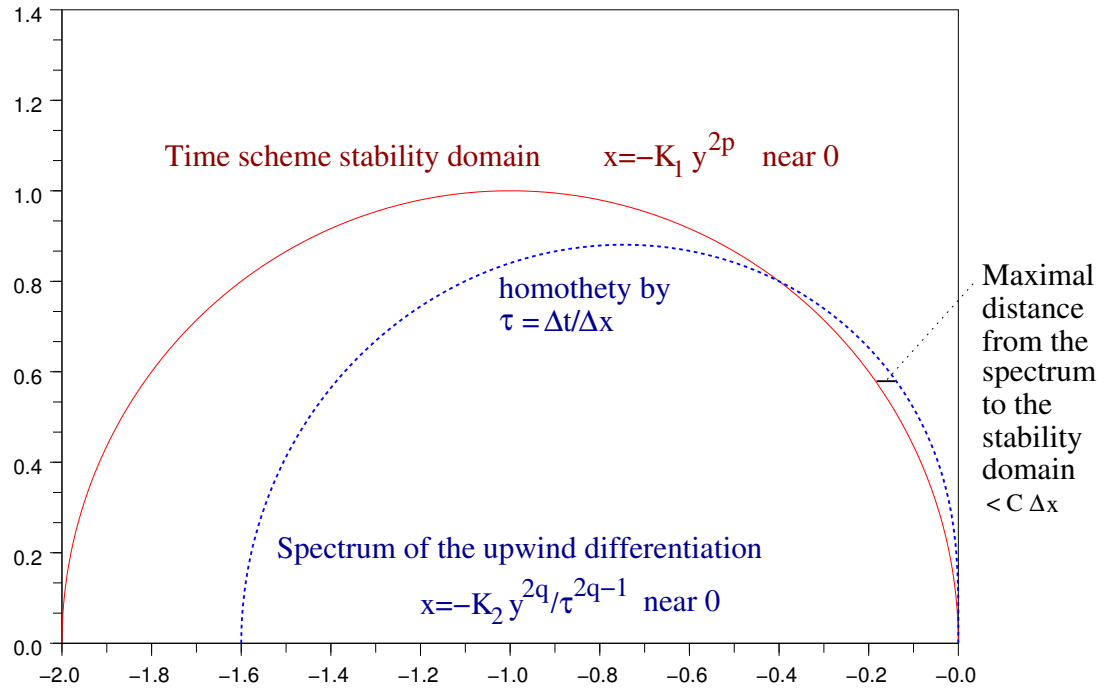

Figure 5: Stability domain $\mathcal{D}$ of the time scheme and spectrum $\mathcal{S}$ of the discretized finite difference space operator.

As all the terms $a^{m+1}b^n$ are negligible with respect to a for $m+n>0$, then

$$
\begin{aligned}
|G(a+i\,b)|^2 &= |1+(a+i\,b)+\beta_2(i\,b)^2+\beta_3(i\,b)^3+\dots|^2+o(a) && (3.10)\\
&= (1+a-\beta_2 b^2+\beta_4 b^4+\dots)^2+(b-\beta_3 b^3+\dots)^2+o(a) && (3.11)\\
&= 1+2a+(1-2\beta_2)b^2+\dots+\left(\sum_{j=0}^{2\ell}(-1)^{\ell+j}\beta_j\beta_{2\ell-j}\right)b^{2\ell}+\dots && (3.12)\\
&= 1+2a+2T_{\mathcal{D}}b^{2p}+o(a)+o(b^{2p}) && (3.13)
\end{aligned}
$$

Now, using the fact that $a=-T_{\mathcal{S}}\tau\,\xi^{2q}+o(\tau\,\xi^{2q})$, $\xi\in[-\pi,\pi]$, and $b=\tau\,\xi+o(\tau\,\xi)$, we look for the maximal value of:

$$
f(\tau,\xi)=1-2T_{\mathcal{S}}\tau\,\xi^{2q}+2T_{\mathcal{D}}\tau^{2p}\xi^{2p}=|G(\tau A(\xi))|^2+o(\tau\,\xi^{2q})+o(\tau^{2p}\xi^{2p}) \qquad (3.14)
$$

This maximum is reached for

$$
\xi=\xi_0=\left(\frac{p\,T_{\mathcal{D}}}{q\,T_{\mathcal{S}}}\right)^{\frac{1}{2(q-p)}}\tau^{\frac{2p-1}{2(q-p)}} \qquad (3.15)
$$

then

$$
|G(\tau\,A(\xi_0))|^2=1+2\frac{T_{\mathcal{D}}^{\frac{q}{q-p}}}{T_{\mathcal{S}}^{\frac{p}{q-p}}}\left(\left(\frac{p}{q}\right)^{\frac{p}{q-p}}-\left(\frac{p}{q}\right)^{\frac{q}{q-p}}\right)\tau^{\frac{p(2q-1)}{q-p}}+o(\tau^{\frac{p(2q-1)}{q-p}}). \qquad (3.16)
$$

Hence, knowing that $\tau = \frac{\Delta t}{\Delta x}$, the von Neumann stability condition $|G(\tau\, A(\xi_0))|^2 \leq 1 + 2C\,\Delta t$ is given by

$$\left(\frac{\Delta t}{\Delta x}\right)^{\frac{p(2q-1)}{q-p}} \leq C \frac{T_{\mathcal{S}}^{\frac{p}{q-p}}}{T_{\mathcal{D}}^{\frac{q}{q-p}}} \left(\left(\frac{p}{q}\right)^{\frac{p}{q-p}} - \left(\frac{p}{q}\right)^{\frac{q}{q-p}} \right)^{-1} \Delta t \tag{3.17}$$

i.e. by the condition $\Delta t \leq C'\,\Delta x^{\alpha}$ (3.4) with $\alpha = \frac{p(2q-1)}{(2p-1)q}$ and C' given by (3.5).

4 Numerical experiment

We test the stability predictions (3.4) of theorem 3.1 on the simplest case of hyperbolic equation. On the interval $[0,1]$ with periodic boundary conditions, we simulate the transport of a function $f : [0,1] \to \mathbb{R}$ by a constant speed, i.e. we solve $\partial_t u = -\partial_x u$ for $(t,x) \in [0,5] \times [0,1]$ where

$$\begin{array}{rl} u : [0,5] \times [0,1] & \to \mathbb{R} \\ (t,x) & \mapsto u(t,x) \end{array}$$

with initial condition $u(0,x) = f(x)$ and periodic boundary condition $u(t,0) = u(t,1)$. During this process, the function f makes five laps, and the exact solution at time $t = 5$ is: $u(5,x) = f(x)$.

This (rather simple) experiment accounts of numerous simulations where the transport dominates the stability properties of the numerical solution. We apply an explicit scheme of Runge-Kutta type with time step Δt to the PDE $\partial u = F\,u$:

$$u_{n+1} = u_n + b_1 \Delta t\, F\left(u_n + b_2 \Delta t\, F\left(u_n + \ldots b_{s-1} \Delta t\, F\left(u_n + b_s \Delta t\, F\, u_n\right)\ldots\right)\right) \tag{4.1}$$

where the parameters $(b_r)_{1 \leq r \leq s}$ are chosen according to the desired amplification factor. The coefficients β_ℓ of the amplification factor (3.6) are given by:

$$\beta_\ell = \prod_{k=1}^{\ell} b_k.$$

We couple this time integration with the finite differences from subsection 2.1. And we use the spacing $\Delta x = \frac{1}{N}$ between the N points of the discretization. So it allows to observe the effects of the parameters p –regarding the time integration– and q –regarding the finite differences– on the stability condition $\Delta t_{\max}(\Delta x)$ and to evidence the exponents of table 3.

For the numerical experiments, we will be using order two Runge-Kutta schemes which maximize p and whose coefficients are given by table 2.

We simulate the transport of the function $f(x) = x$ which presents a discontinuity at $x = 0$ by a constant velocity. Then, in Fig. 6, we represent the Fourier transform of the numerical solution at time $t = 5$ obtained using the Runge-Kutta order two integration scheme in conjunction with several finite difference approximations. Three typical cases appear, using a linear CFL condition:
- the numerical scheme is stable but the high frequencies are dumped, e.g. Runge-Kutta 2 with an upwind order two ($p = 2$ and $q = 2$, see Fig. 7), or every Runge-Kutta 3 or 4,

p \ r	1	2	3	4
1	1			
2	1	$\frac{1}{2}$		
3	1	$\frac{1}{2}$	$\frac{1}{4}$	
4	1	$\frac{1}{2}$	$\frac{2-\sqrt{2}}{2}$	$\frac{2-\sqrt{2}}{4}$

Table 2: Table of coefficients b_r forming the numerical schemes (4.1) with parameters $p = 1, 2, 3, 4$ regarding the tangency property (3.1).

p \ q	1	2	3	4	5	$+\infty$
1	1	$\frac{3}{2}$	$\frac{5}{3}$	$\frac{7}{4}$	$\frac{9}{5}$	2
2	1	1	$\frac{10}{9}$	$\frac{7}{6}$	$\frac{6}{5}$	$\frac{4}{3}$
3	1	1	1	$\frac{21}{20}$	$\frac{27}{25}$	$\frac{6}{5}$
4	1	1	1	1	$\frac{36}{35}$	$\frac{8}{7}$

Table 3: Table of exponents $\alpha = \frac{p(2q-1)}{q(2p-1)}$ for the non linear CFL stability condition (3.4).

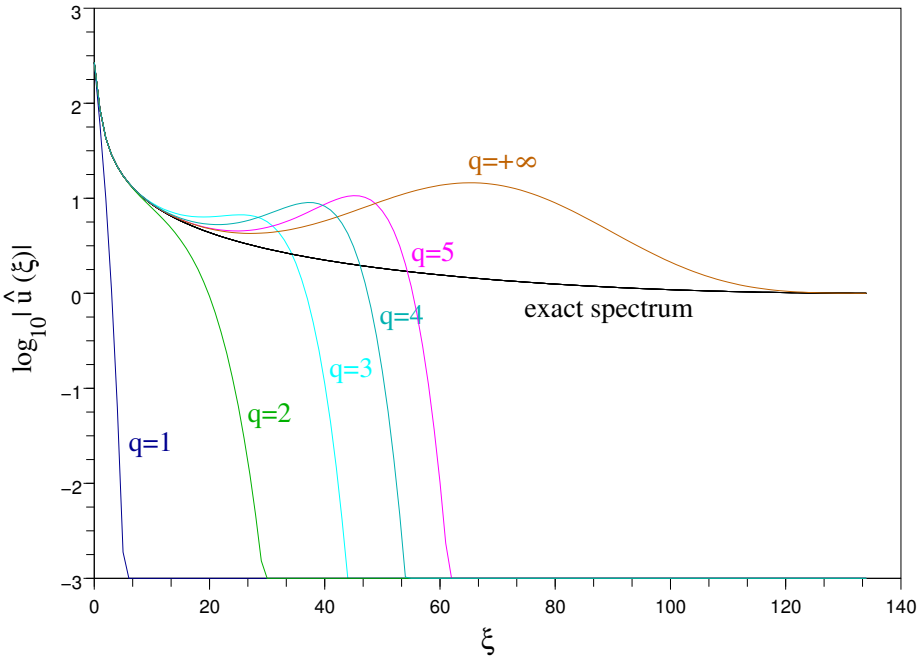

Figure 6: Fourier transform $\hat{u}(5,\xi)$ of the numerical solution obtained with a Runge-Kutta 2 time scheme and various finite difference differentiations: upwind schemes of orders 1, 3, 5, 7 and 9 ($q = 1, 2, 3, 4, 5$), and centered scheme ($q = +\infty$).

- an instability occurs at high frequency $\xi = \pi\frac{N}{2}$, e.g. Euler or Runge-Kutta 2 in association with centered finite differences (see Fig. 8),
- an instability occurs at low frequency $\xi = C\,N^{-1/2q}\,N$, $q \geq 2$ (see Fig. 6), e.g. Euler with upwind of order two, Runge-Kutta 2 with upwind of order greater or equal to four (see Fig. 7 and 8). It can be checked that an order $2n$ scheme has a tangency parameter q at least equal to $n+1$ as indicated in the proof of [5] Theorem 3.2.

In Fig. 6, 7 and 8, the number of points was chosen equal to $N = 271$, and the time step equal to $\frac{5}{6}\Delta t_{\max}$ with $\Delta t_{\max}$ coming from the second experiment equation (4.2).

In Fig. 6 we can observe the spectra of the transported function with six different finite-difference schemes. The corresponding physical results are plotted in Fig. 7 and 8. We remark that all the numerical solutions present spurious oscillations except when using the upwind order one differentiation. While the centered finite differences allow the best conservativity as seen in Fig. 6, they also alter the aspect of the solution dramatically as seen in Fig. 8, whatever explicit time scheme we choose. This is due to the Gibbs phenomenon and is not related to any stability issue.

Now, let us check the relevance of the stability condition (3.4). For different space steps $\Delta x = \frac{1}{N}$, we compute the maximal time steps $\Delta t_{\max}$ such that

$$\forall \Delta t \leq \Delta t_{\max}, \quad \forall n \leq \frac{5}{\Delta t}, \quad \|u_n\|_{\mathrm{TV}} \leq 4\,\|u_{\frac{1}{\Delta t}}\|_{\mathrm{TV}}. \tag{4.2}$$

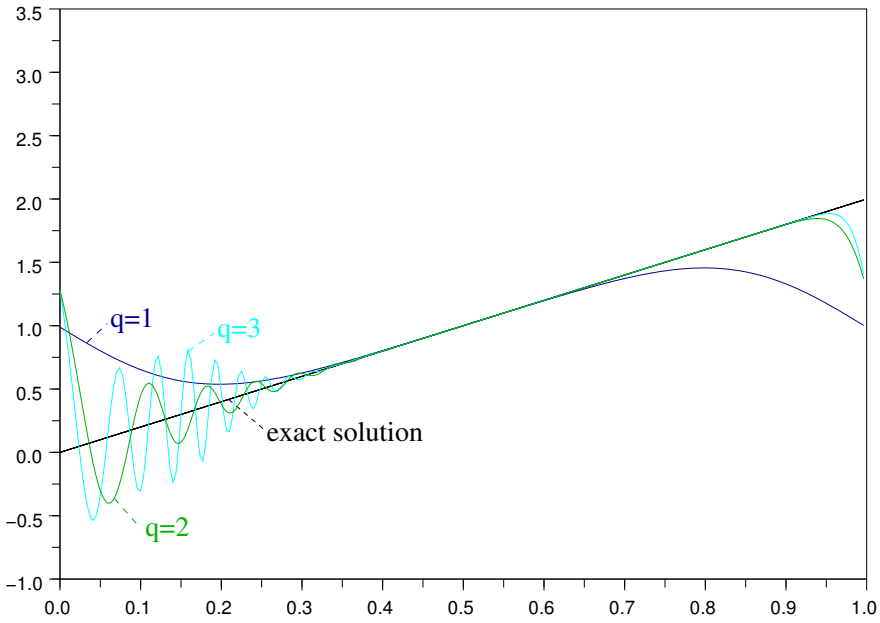

Figure 7: Physical result of the transport of a discontinuous function using Runge-Kutta 2 and upwind of orders 1, 3 and 5 finite differences ($q = 1, 2, 3$) after five loops: $u(5, x)$.

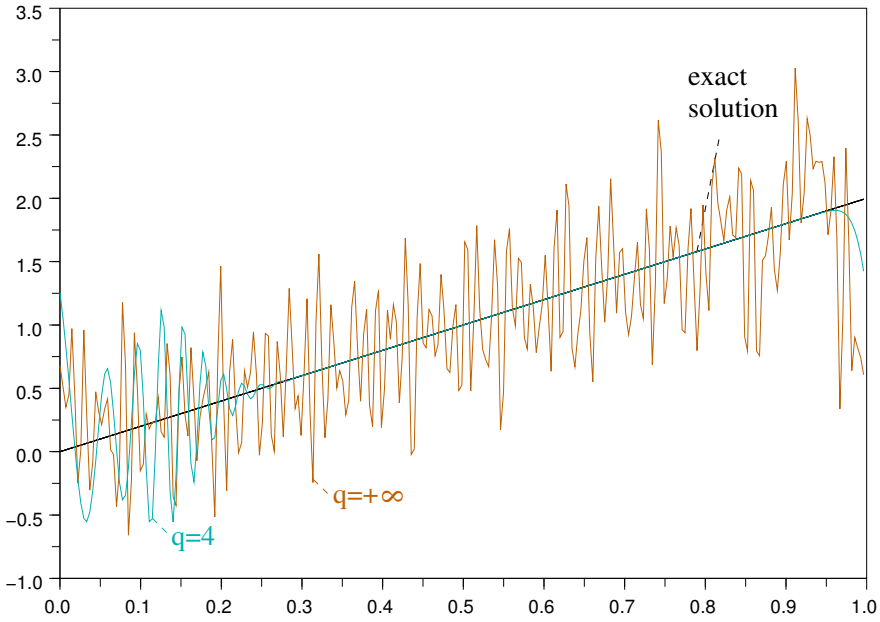

Figure 8: Physical result of the transport of a discontinuous function using Runge-Kutta 2 and upwind of order 7 ($q = 4$) and centered finite difference ($q = +\infty$).

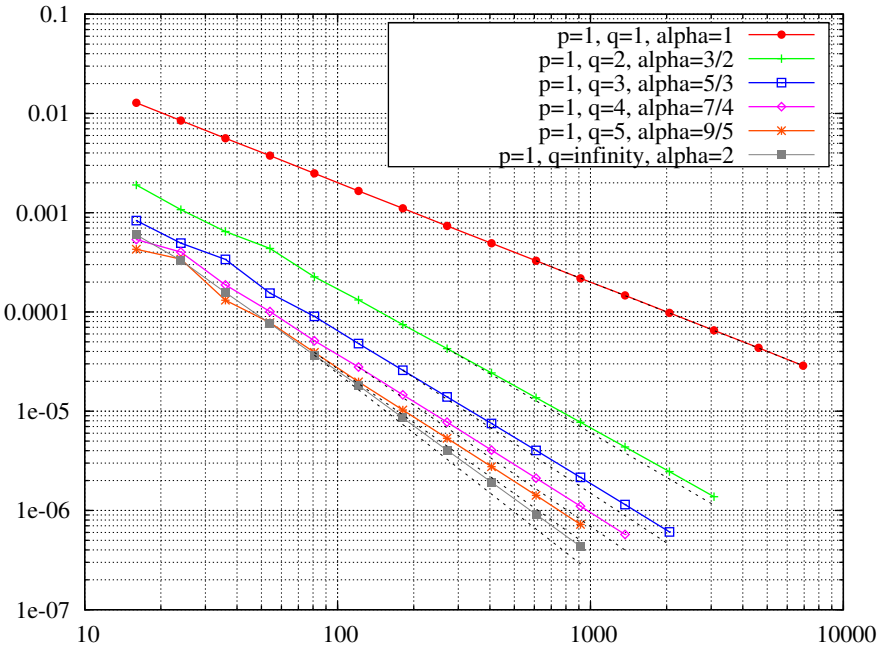

Figure 9: Numerical experiment with $p = 1$ and various q. The (Ox) axis figures the number N of points in the space discretization, the (Oy) axis, the time step $\Delta t_{\max}$ in log-scale. The dotted lines represent the theoretical slopes $\Delta t = O(N^{-\alpha})$.

where the constant 4 is arbitrary, and the solution at time $t = 1$, $u_{\frac{1}{\Delta t}}$ chosen so that the Gibbs phenomenon does not interfere with stability issues.

We plot the results for various values of p and q in Fig. 9, 10 and 11, taking as an initial condition the continuous function:

$$f(x) = \begin{cases} 5x \quad \text{for} \quad x \leq \frac{1}{5}, \\ 2 - 5x \quad \text{for} \quad x \in]\frac{1}{5}, \frac{2}{5}], \\ 0 \quad \text{for} \quad x > \frac{2}{5} \end{cases} \tag{4.3}$$

This experiment corroborates our approach: although the initial condition and the divergence criterion influence the slopes –i.e. the exponent α–, these are located only slightly above the predicted ones, and their relative positions fit our perditions very well (Fig. 9, 10 and 11).

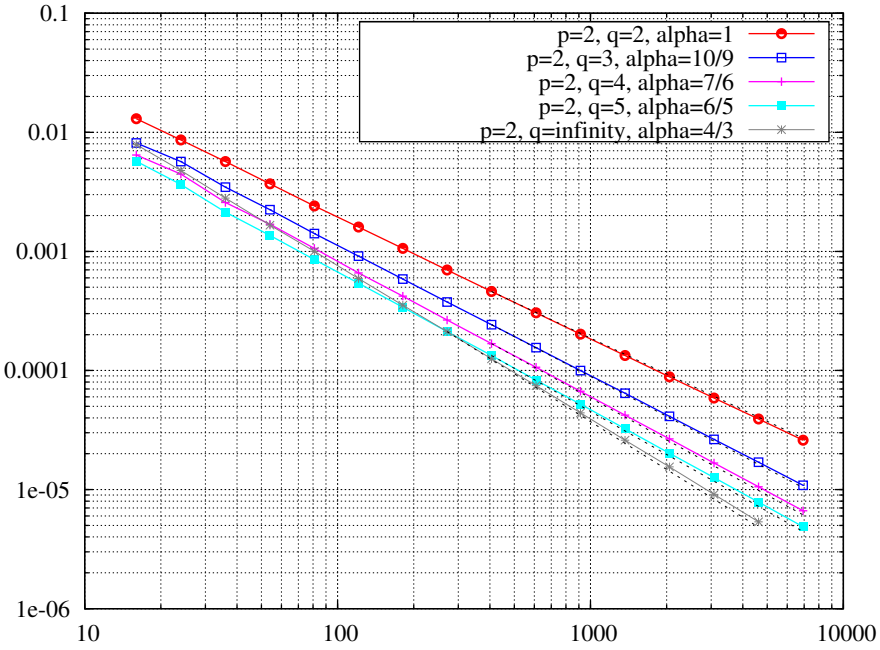

Figure 10: Numerical experiment with $p = 2$ and various q.

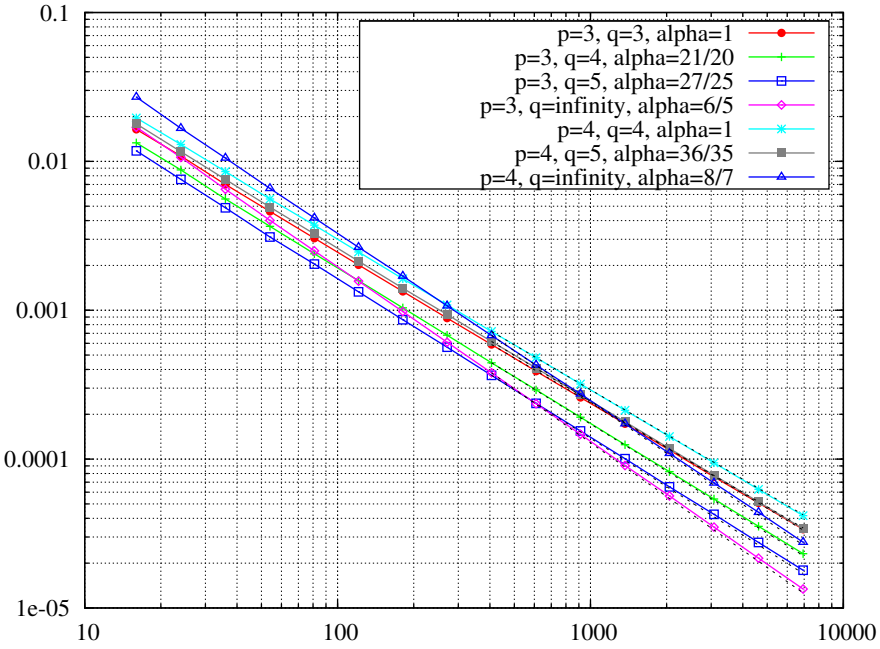

Figure 11: Numerical experiment with $p = 3, 4$ and various q.

Conclusion

The present paper completes the previous paper [5] by proving and testing the upwind Von Neumann stability condition: $\Delta t \leq C\,\Delta x^{\alpha}$ with $C > 0$ and $\alpha \in [1, 2]$ explicited.

The numerical simulation community is already intuitively aware of the containt of this paper [12], although our precise stability assertions –Theorem 3.1– had not been clearly established earlier [11, 15]. These results help to select a time integration scheme: for instance for someone using an upwind of order two, its is useless –from the stability point of view– to go higher than the order two for the time integration. They also explain some possible instabilities appearing in explicit hyperbolic numerical simulations: at high frequencies using centered discretizations [12], and at low frequencies for upwind schemes [2].

The numerical experiments meet our predictions more or less accurately.

References

[1] J.G. Charney, R. Fjörtoft, J. von Neumann, *Numerical Integration of the Barotropic Vorticity Equation*, Tellus Vol. 2, pp 237–254, 1950.

[2] Bernardo Cockburn, George E. Karniadakis, Chi-Wang Shu (Eds.), *Discontinuous Galerkin Methods: Theory, Computation and Applications*, Springer 2000.

[3] R. Courant, K. Friedrichs, H. Lewy, *On the Partial Difference Equations of Mathematical Physics*, IBM Journal, march 1967, translation from a paper originally appeared in *Mathematische Annalen* **100**, 32–74, 1928.

[4] M. Crouzeix, A.L. Mignot, *Analyse numérique des équations différentielles*, Masson editor, 1992.

[5] E. Deriaz, *Stability conditions for the numerical solution of convection-dominated problems with skew-symmetric discretizations*, SIAM J. Numer. Anal. **50**(3) 1058–1085, 2012.

[6] E. Deriaz and D. Kolomenskiy, *Stabilité sous condition CFL non linéaire*, ESAIM: Proc. **35** 114–121, 2012.

[7] E. Godlewski, P.A. Raviart, *Numerical Approximation of Hyperbolic Systems of Conservation Laws*, Springer 1996.

[8] Ernst Hairer, Syvert Paul Nørsett, Gerhard Wanner, *Solving Ordinary Differential Equations I. Nonstiff Problems.* Springer Series in Comput. Mathematics, Vol. 8, Springer-Verlag 1987, Second revised edition 1993.

[9] Ernst Hairer, Gerhard Wanner, *Solving Ordinary Differential Equations II. Stiff and Differential-Algebraic Problems.* Springer Series in Comput. Mathematics, Vol. 14, Springer-Verlag 1991, Second revised edition 1996.

[10] A.N. Kolmogorov, A.P. Yushkevich (Eds.), *Mathematics of the 19th Century*, Vol. III, 1998.

[11] D. Levy and E. Tadmor, *From Semidiscrete to Fully Discrete: Stability of Runge–Kutta Schemes by The Energy Method*, SIAM Review **40**(1) 40–73, 1998.

[12] M. Mohan Rai and P. Moin, *Direct simulations of turbulent flow using finite-difference schemes*, J. Comput. Phys. **96**(1) 15–53, 1991.

[13] R. Peyret, *Spectral methods for incompressible viscous flow* (Vol. 148), Springer, 2002.

[14] Lloyd N. Trefethen, *Finite Difference and Spectral Methods for Ordinary and Partial Differential Equations*, unpublished text, 1996, available at http://people.maths.ox.ac.uk/trefethen/pdetext.html

[15] P. Wesseling, *Principles of Computational Fluid Dynamics*, Berlin et al., Springer-Verlag 2001.